$\pi^- p$ Two-Prong Interactions at 4.16 GeV/c*

R. L. EISNER, P. B. JOHNSON, P. R. KLEIN, R. E. PETERS, R. J. SAHNI, W. L. YEN,
AND G. W. TAUTFEST

Department of Physics, Purdue University, Lafayette, Indiana

(Received 5 July 1967)

An analysis of $\pi^- p$ two-prong interactions at 4.16 GeV/c is presented. The total two-prong cross section is 19.11±0.40 mb, based on 33 672 events. The elastic-scattering differential cross section shows an exponential behavior, $K \exp(-A\Delta^2)$. With $A = 7.36\pm0.14$ GeV^{-2}, the "absorption parameters" are derived as $C_+ = 0.846\pm0.017$ and $\gamma_+ = 0.040\pm0.001$. The final-state $\pi^-\pi^0 p$ exhibits a strong ρ^-, and the $\pi^-\pi^+ n$ a strong ρ^0 and f^0. The partial cross sections for the dominant resonant channels $p\rho^-$, $\pi^-\Delta^+(1236)$ $(\rightarrow p\pi^0)$, $\rho^0 n$, and $f^0 n$ are 0.59±0.03, 0.17±0.01, 1.15±0.05, and 0.53±0.06 mb, respectively. The ρ^- production and decay angular distributions do not agree with the predictions of the absorption-modified one-pion-exchange model. However, an inclusion of the contribution from ω exchange adequately accounts for the discrepancy. The ρ^0 asymmetry is interpreted as a result of an interference of the resonant P wave and isospin-zero S wave, and the corresponding spin-density matrix elements are obtained. In the final state $\pi^- p +$neutrals, a clear peak for the η meson and some evidence for the ω meson are seen.

I. INTRODUCTION

SEVERAL laboratories have undertaken the study of $\pi^- p$ two-prong interactions at a number of beam momenta.[1-11] The dominance of ρ production has been a common feature. In many of these experiments attempts have been made to fit the ρ-meson production and decay angular distributions to the predictions of the absorption-modified one-pion-exchange model (OPEA).[12-15] The major limitation to such comparisons has been the poor statistics in many of these investigations.

This experiment represents a significantly larger sample to carry out a more detailed comparison with OPEA. The data were obtained from an exposure of the Lawrence Radiation Laboratory 72-in. hydrogen bubble chamber to a beam of 4.16-GeV/c π^- mesons. The reactions considered are:

$$\pi^- p \rightarrow \pi^- \pi^0 p, \tag{1}$$

$$\pi^- p \rightarrow \pi^- \pi^+ n, \tag{2}$$

$$\pi^- p \rightarrow \pi^- p, \tag{3}$$

$$\pi^- p \rightarrow \pi^- p + \text{neutrals}, \tag{4}$$

$$\pi^- p \rightarrow \pi^- \pi^+ + \text{neutrals}. \tag{5}$$

Preliminary reports on this experiment have been presented earlier.[16] The contribution of ω exchange to the production of ρ^- in reaction (1)[17] and the determination of the $\pi\pi$ S-wave phase shifts[18] have been discussed separately.
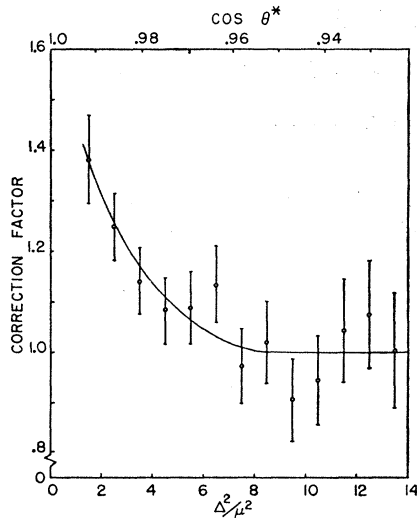
II. EXPERIMENTAL DETAILS

Scanning nearly 52 000 pictures, we find a total of 44 172 events with two charged secondaries. The events were measured on two digitizing microscopes and three SMP's (scanning and measuring projectors) on line to an IBM 7044. The geometric reconstruction and kinematic fitting was also performed on an IBM 7044 using the University of California Radiation Laboratory programs PANAL and PACKAGE. Five hypotheses represented by reactions (1) to (5) were attempted by PACKAGE.

* Work supported in part by the U. S. Atomic Energy Commission.

[1] L. D. Jacobs, University of California Radiation Laboratory Report No. UCRL-16877, 1966 (unpublished).

[2] Saclay-Orsay-Bari-Bologna Collaboration, Nuovo Cimento 29, 515 (1963).

[3] E. West, J. H. Boyd, A. R. Erwin, and W. D. Walker, Phys. Rev. 149, 1089 (1966).

[4] Vasken Hagopian and Yu-Li Pan, Phys. Rev. 152, 1183 (1966).

[5] Saclay-Orsay-Bari-Bologna Collaboration, Nuovo Cimento 35, 713 (1965).

[6] V. Hagopian, W. Selove, J. Alitti, J. P. Baton, and M. Neveu-René, Phys. Rev. 145, 1128 (1966).

[7] D. H. Miller, L. Gutay, P. B. Johnson, F. J. Loeffler, R. L. McIlwain, R. J. Sprafka, and R. B. Willmann, Phys. Rev. 153, 1423 (1967).

[8] Aachen-Birmingham-Bonn-Hamburg-London (I.C.)-München Collaboration, Nuovo Cimento 31, 729 (1964).

[9] G. Goldhaber, in *Proceedings of the Thirteenth Annual International Conference on High-Energy Physics, Berkeley, California, 1966* (University of California Press, Berkeley, 1967), p. 103.

[10] D. J. Crennell, P. V. C. Hough, G. R. Kalbfleisch, K. W. Lai, J. M. Scarr, T. G. Schumann, I. O. Skillicorn, R. C. Strand, M. S. Webster, P. Baumel, A. H. Bachman, and R. M. Lea, Phys. Rev. Letters 18, 323 (1967).

[11] I. Derado, J. A. Poirier, N. N. Biswas, N. M. Cason, V. P. Kenney, and W. D. Shephard, Phys. Letters 24B, 112 (1967).

[12] K. Gottfried and J. D. Jackson, Nuovo Cimento 34, 735 (1964); J. D. Jackson, Rev. Mod. Phys. 37, 484 (1965); J. D. Jackson, J. T. Donohue, K. Gottfried, R. Keyser, and B. E. Y. Svensson, Phys. Rev. 139, B428 (1965).

[13] M. H. Ross and G. L. Shaw, Phys. Rev. Letters 12, 627 (1964).

[14] L. Durand and Y. T. Chiu, Phys. Rev. 137, B1530 (1965).

[15] J. G. Wills, D. Ellis, and D. B. Lichtenberg, Phys. Rev. 143, 1375 (1966).

[16] T. H. Groves, P. R. Klein, T. R. Palfrey, and R. J. Sahni, Bull. Am. Phys. Soc. 11, 55 (1966); R. E. Peters, R. L. Eisner, P. B. Johnson, P. R. Klein, R. J. Sahni, and W. L. Yen, *ibid.* 12, 10 (1967); P. B. Johnson, L. J. Gutay, R. L. Eisner, R. E. Peters, R. J. Sahni, and W. L. Yen, *ibid.* 12, 10 (1967).

[17] W. L. Yen, R. L. Eisner, L. Gutay, P. B. Johnson, P. R. Klein, R. E. Peters, R. J. Sahni, and G. W. Tautfest, Phys. Rev. Letters 18, 1091 (1967).

[18] P. B. Johnson, L. J. Gutay, R. L. Eisner, P. R. Klein, R. E. Peters, R. J. Sahni, W. L. Yen, and G. W. Tautfest (to be published).

FIG. 1. Correction factor F for elastic scattering.

pared, respectively, to 2368 and 2912 events with $p_+ < 1300$ MeV/c. Furthermore, there are 817 events ambiguous between (1) and (2) (this number contains 39 events with $p_+ < 1300$ MeV/c which were not resolved on visible ionization estimates). We could not find any satisfactory way of assigning them individually to either hypothesis. Their exclusion from the sample is also objectionable, for it can cause biases in certain angular distributions. For instance, the exclusion of these events from hypothesis (2) will cause an artificial asymmetry in the ρ^0 decay. Thus, we chose to assign them on the basis of X^2. The effective-mass distributions of the events, assigned this way, are not very much different from those obtained from the respective unambiguous samples.

The PACKAGE output, for each event, was tested for measurement quality and fiducial volume restrictions. The events which failed measurement-quality tests were remeasured; however, no event was measured more than three times. There are 2939 events which failed all three measurements. These events have been excluded from the sample without introducing any biases. From the remaining 41 233 measured events, 7561 were outside the fiducial volume.
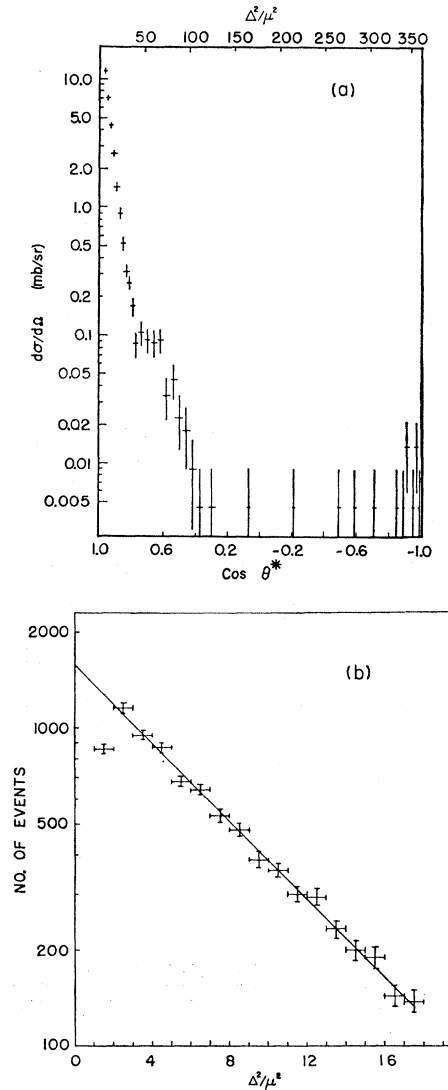
A total of 33 672 events which lay within the fiducial volume and also passed the reconstruction tests were assigned on the basis of X^2 to one or more of the hypotheses (1) to (5). The X^2 limits, chosen for this experiment, correspond to probabilities of $\sim 10^{-2}$ and $\sim 2\%$ for four-constraint and one-constraint fits, respectively. If an event was ambiguous between hypothesis (3) and hypothesis (1) or (2), it was accepted as (3) irrespective of the confidence levels of the fits. However, if an event had acceptable fits to hypothesis (1) as well as (2), but not to (3), it was classified as ambiguous between (1) and (2) for all ratios of confidence levels. Those events which did not fit any of the hypotheses (1) to (3) were assigned to (4) and (5).
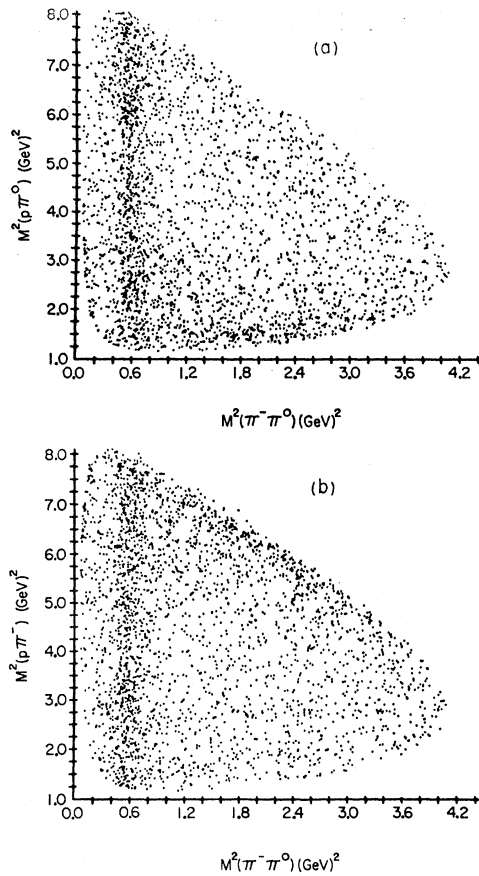
Events which on the basis of X^2 belonged to final states (1), (2), or both, were divided into two groups: one with the momentum of the positive secondary (denoted hereafter as p_+) less than 1300 MeV/c and the other with $p_+ > 1300$ MeV/c. The cutoff, 1300 MeV/c, corresponds to the limit above which visible ionization estimates cannot distinguish between a π^+ and a proton.

The ionization examination of the events with p_+ < 1300 MeV/c revealed that nearly 19% of the (1)'s were (5)'s and about 5% of the (2)'s were (4)'s.

The events with $p_+ > 1300$ MeV/c were treated as follows. Those which on the basis of X^2 fitted uniquely to hypothesis (1) or (2) were assigned accordingly. There are 200 such events for (1) and 982 for (2) com-

FIG. 2. Differential cross section for elastic scattering as a function of $\cos\theta^*$ and Δ^2: (a) for the entire range of Δ^2, (b) restricted only to the diffraction peak. The solid line is a least-squares fit to the data.

FIG. 3. Dalitz plots for the state $\pi^-\pi^0 p$.

Contributions from the various assignments discussed above add up to 2900 events for reaction (1) and 4379 for reaction (2).[19] The analysis presented in Sec. IV is based on these events.

To assign 15 538 zero-constraint fits to hypothesis (4) or (5) a subsample of 5496 events was used. Of these, 4185 events possess $p_+ < 1300$ MeV/c and were examined for ionization identification. It was found that 1246 were consistent with hypothesis (4) and 2939 with (5).

## III. ELASTIC SCATTERING AND CROSS-SECTION NORMALIZATION

In lieu of measuring total path length, we have used elastic-scattering events and the optical theorem to deduce the correspondence between unit cross section and the number of events for this sample.

Out of 33 672 measured events within the fiducial volume, 9584 fit the elastic-scattering hypothesis [reaction (3)]. Since they are four-constraint fits, they

---

[19] A subsample of 1394 events, which on the basis of χ^2 belonged to hypothesis, (1), (2), or both, were not examined for ionization identification. However, they have been included for cross section determination.

form a relatively pure sample. However, there are severe scanning biases for small values of Δ^2, the square of the four-momentum transfer between the incoming and the outgoing nucleon. This bias occurs because of the difficulty in detecting a proton of short projected range and shows up as a depopulation of events when the angle (Φ) between the average camera plane and the production plane approaches 90°. To correct for this bias, the events were divided into several Δ^2 intervals and the corresponding Φ distributions were examined. The regions near 0° and 180° were used to estimate the true number of events and to obtain the correction factor F ($=$ expected number/observed number). The observed dependence of F on Δ^2 is shown in Fig. 1. The errors are statistical, and the curve is a visual fit to the datum points.

Figure 2(a) shows the corrected differential cross section as a function of $\cos\theta^*$, where θ^* is the center-of-mass scattering angle. Figure 2(b) shows the differential cross section for the diffraction peak only. The data are consistent with an exponential behavior, $d\sigma/d\Delta^2 = K \times \exp(-A\Delta^2)$. A least-squares fit [solid line in Fig. 2(b)] over the region $2 < \Delta^2 \le 18\mu^2$, where μ is the mass of a charged pion, yields $K = 1566 \pm 36$ events/μ^2 and
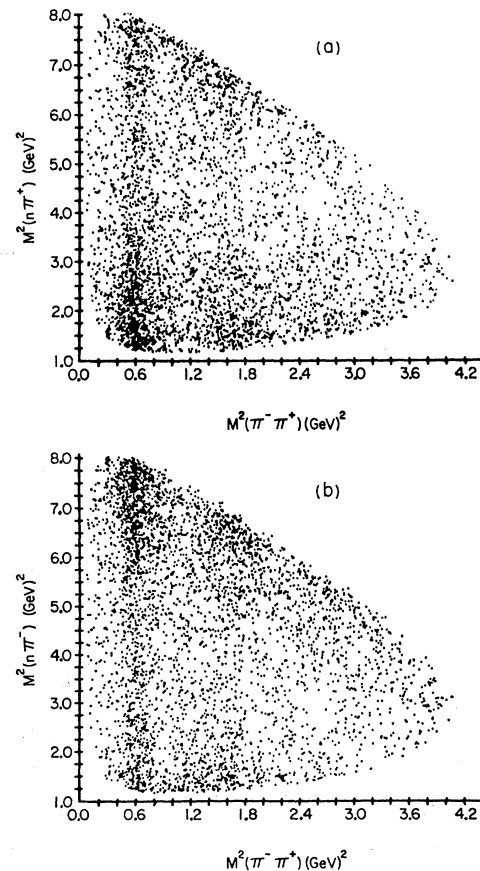
FIG. 4. Dalitz plots for the state $\pi^-\pi^+ n$.

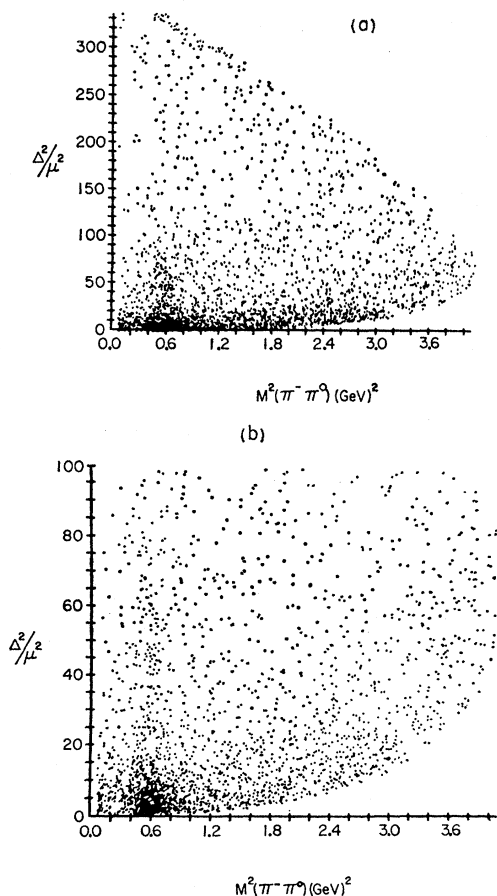FIG. 5. Chew-Low plots for the state $\pi^-\pi^0 p$: (a) all events, (b) events with $\Delta^2 < 100\mu^2$.

$A = 7.36 \pm 0.14$ GeV^{-2}. The value of A is in agreement with those obtained at other energies.[20]

Knowing A, one can calculate the elastic-scattering "absorption parameters"[12] as $C_+ = \sigma_T/(4\pi A) = 0.846 \pm 0.017$ and $\gamma_+ = 1/(2q^2 A) = 0.040 \pm 0.001$, where σ_T and q denote the total cross section and the center-of-mass momentum, respectively. These parameters are used to modify the Born amplitudes in accordance with the absorption model (Sec. IV).

TABLE I. Cross sections for two-prong final states.

Final state	No. of events	Cross section (mb)
$\pi^- p \pi^0$	3403	1.88 ± 0.05
$\pi^- \pi^+ n$	5147	2.85 ± 0.07
$\pi^- p$	10 414[a]	5.77 ± 0.13
$\pi^- p$+neutrals	4533	2.51 ± 0.06
$\pi^- \pi^+$+neutrals	11 005	6.10 ± 0.14

[a] Corrected for scanning biases for low Δ^2.

[20] S. Brandt, V. T. Cocconi, D. R. O. Morrison, A. Wroblewski, P. Fleury, G. Kayas, F. Muller, and C. Pelletier, Phys. Rev. Letters **10**, 413 (1963).

Using the optical theorem, one can derive the relation

$$\left(\frac{d\sigma}{d\Delta^2}\right)_{\Delta^2=0} = \frac{1}{16\pi}[\sigma_T^2(1+\alpha^2)], \qquad (6)$$

where $\alpha = \mathrm{Re}f(0)/\mathrm{Im}f(0)$. With $(d\sigma/d\Delta^2)_{\Delta^2=0} = K = 1566 \pm 36$ events/μ^2, $\alpha = -0.18$,[21] and $\sigma_T = 30.30$ mb [22] in Eq. (6), the correspondence between the number of events and the unit cross section is: 1 event $= 0.5539 \pm 0.0120 \mu$b.

This gives a total cross section of 19.11 ± 0.40 mb for the two-prong interactions at 4.16 GeV/c. The cross sections for each of the final states (1) to (5) are presented in Table I. The errors quoted are a combination of the statistical errors and the error in the event normalization. For the final states (1) and (2) there is a further uncertainty due to possible misassignment of events with $p_+ > 1300$ MeV/c. In the case of elastic
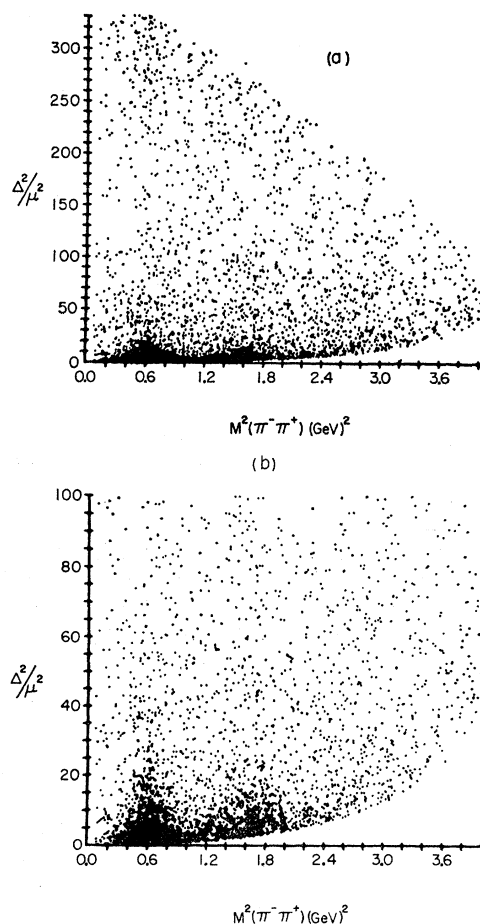

FIG. 6. Chew-Low plots for the state $\pi^-\pi^+ n$: (a) all events, (b) events with $\Delta^2 < 100\mu^2$.

[21] A. A. Nomofilov, I. M. Sitnik, L. A. Slepets, L. N. Strunov, and L. S. Zolin, Phys. Letters **22**, 350 (1966); V. S. Barashenkov, ibid. **19**, 699 (1966).

[22] A. Citron, W. Galbraiter, T. F. Kycia, B. A. Leontic, R. H. Phillips, A. Rousset, and P. H. Sharp, Phys. Rev. **144**, 1101 (1966).
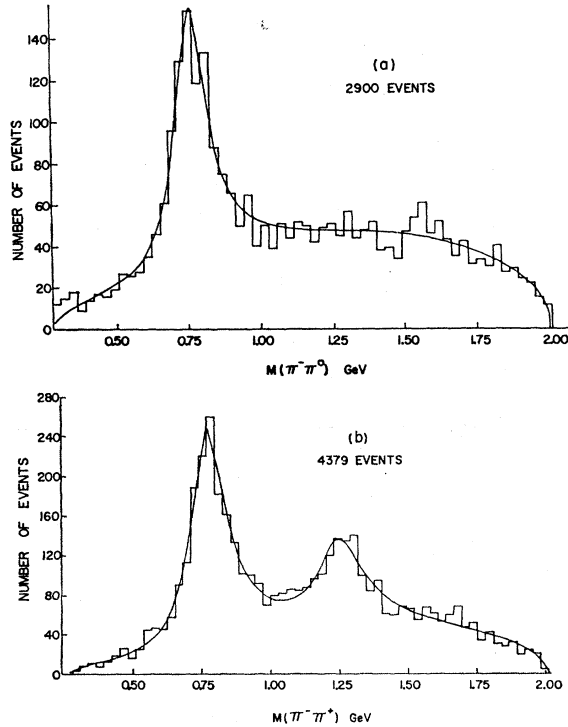
FIG. 7. $\pi\pi$ effective-mass spectra: (a) $\pi^- p \to \pi^- \pi^0 p$, (b) $\pi^- p \to \pi^- \pi^+ n$.

scatterings [reaction (3)], an 8.7% correction has been made for the loss of events at small scattering angles. The numbers for (4) and (5) include 3530 events with $p_+ > 1300$ MeV/c, assigned in proportion to the events in these channels with $p_+ < 1300$ MeV/c.

IV. THE FINAL STATES $\pi^- \pi^0 p$ AND $\pi^- \pi^+ n$

A. Resonance Production

This section is devoted to the study of final states (1) and (2) based on the analysis of 2900 and 4379 events, respectively. The details of the selection of these events are discussed in Sec. II.

Two Dalitz plots for reaction (1) are shown in Fig. 3. The presence of ρ^- in both plots is very striking. There is also an enhancement in the region of $\Delta^+(1236)$. Figure 4 shows similar plots for reaction (2) and exhibits strong ρ^0 and f^0 signals. The decay asymmetry of the ρ^0 manifests itself as different population of events in the ρ^0 band for the two halves of the Dalitz plot.

The Chew-Low plots are shown in Figs. 5 and 6. They depict the fact that the production of the ρ and f^0 is concentrated at low values of Δ^2. Even outside the regions of the ρ and f^0 one observes a general concentration of events along the lower edge of the plots. This illustrates that reactions (1) and (2), at these energies, are dominated by peripheral processes.

The $\pi\pi$ effective-mass distributions for both charged states are shown in Fig. 7. To determine the cross sec-
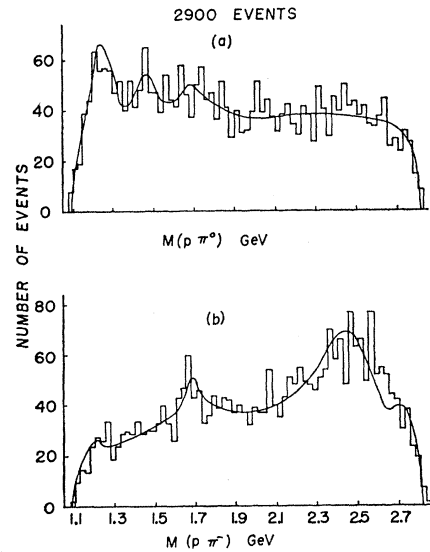

FIG. 8. πN effective-mass plots for the reaction $\pi^- p \to \pi^- \pi^0 p$: (a) $\pi^0 p$, (b) $\pi^- p$.

tions of ρ and f^0 mesons from these plots, the energy-dependent expressions[23]

$$\varphi_R(\omega) = \frac{\omega}{q} \frac{\Gamma(\omega)}{(\omega_0^2 - \omega^2)^2 + \omega_0^2 \Gamma^2(\omega)},$$ (7)

and

$$\Gamma(\omega) = \Gamma_0 (q/q_0)^{2l+1} (\omega_0/\omega)$$ (8)

were used for the Breit-Wigner shape and the width of

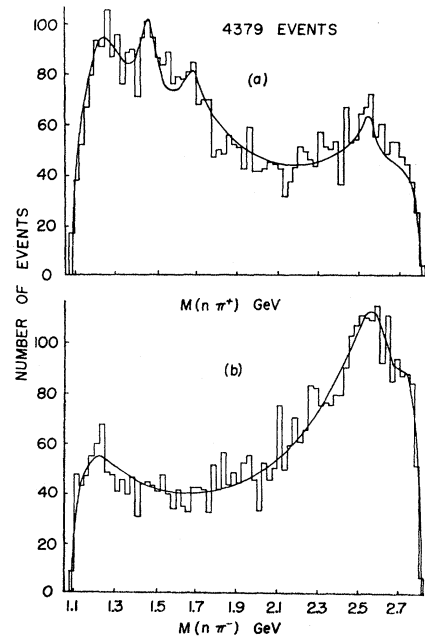FIG. 9. πN effective-mass plots for the reaction $\pi^- p \to \pi^- \pi^+ n$: (a) $\pi^+ n$, (b) $\pi^- n$.

[23] J. D. Jackson, Nuovo Cimento 34, 1644 (1964).

(a)

$M(\pi^-\pi^0)$ GeV
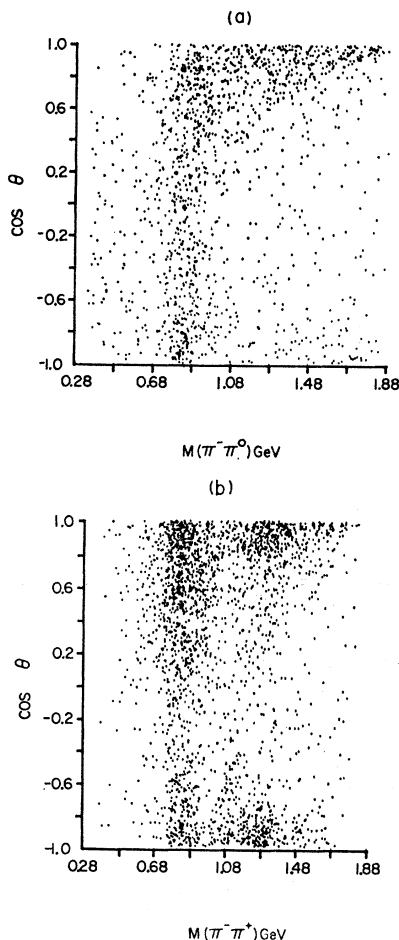
(b)

$M(\pi^-\pi^+)$ GeV

FIG. 10. $\pi\pi$ invariant mass versus $\cos\theta$ for $\Delta^2 \leq 20\mu^2$:
(a) $\pi^-\pi^0 p$, (b) $\pi^-\pi^+ n$.

each resonance. In expressions (7) and (8), ω is the $\pi\pi$ invariant mass, q is the 3-momentum of either pion in the dipion rest frame, ω_0 is the mass of the resonance, and Γ_0 and q_0 are the values of Γ and q at $\omega = \omega_0$. The symbol l denotes the relative orbital angular momentum of the two pions in their rest frame.

The $\pi^-\pi^0$ spectrum was fitted to an incoherent superposition of phase space and a P-wave Breit-Wigner shape (using the above expressions), whereas the fit to the $\pi^-\pi^+$ spectrum included, in addition, a D-wave Breit-Wigner shape. The values of ω_0, Γ_0, and the fraction of each resonance were obtained from a maximum-

TABLE II. Parameters of fits to masses and widths of ρ^-, ρ^0, and f^0 in MeV.

Reso-nance	All Δ^2		$\Delta^2 < 20\mu^2$		$\Delta^2 < 10\mu^2$	
	ω_0	Γ_0	ω_0	Γ_0	ω_0	Γ_0
ρ^-	764±4	133±11	765±4	146±13	767± 5	131±12
ρ^0	781±3	166±11	780±4	186±13	780± 4	179±15
f^0	1271±9	219±39	1264±7	173±25	1263±10	183±40

likelihood analysis of each dipion spectrum. For instance, the analysis of the $\pi^-\pi^+$ spectrum involves six unknown parameters; the fraction, the mass ω_0, and the width Γ_0 of both ρ^0 and f^0. The curves in Fig. 7 show the best fits to the data. They represent $(31.0\pm1.7)\%$ ρ^- and $(69.0\pm1.7)\%$ phase space for $\pi^-\pi^0$ [$P(\chi^2)=52\%$], and $(40.4\pm1.6)\%$ ρ^0, $(18.6\pm1.9)\%$ f^0 and $(41.0\pm2.5)\%$ phase space for $\pi^-\pi^+$ [$P(\chi^2)=36\%$]. The values of ω_0 and Γ_0 obtained from these fits are given in Table II. Also given in Table II is their dependence on Δ^2 cuts. It must be pointed out that ω_0 is not the observed peak position of the resonance and there can be an appreciable difference between the two.[23]

It is obvious that the production of a strong non-isotropically decaying resonance in the $\pi\pi$ state causes serious distortions of the πN phase space. To estimate these distortions (or reflections), three samples of simulated events for the reactions $\pi^-p \to \rho^-p$, $\pi^-p \to \rho^0 n$, and $\pi^-p \to f^0 n$ were generated using a Monte Carlo program. For the production and the decay of the resonance the experimental distributions were used. From these simulated events the πN effective masses
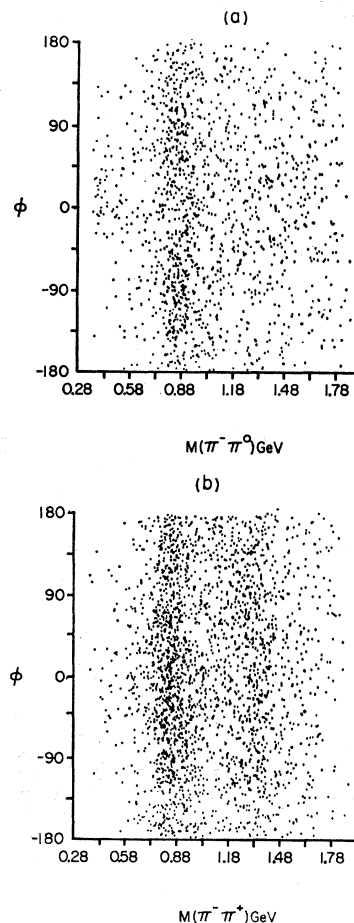
(a)

$M(\pi^-\pi^0)$ GeV

(b)

$M(\pi^-\pi^+)$ GeV

FIG. 11. $\pi\pi$ invariant mass versus φ for $\Delta^2 \leq 20\mu^2$:
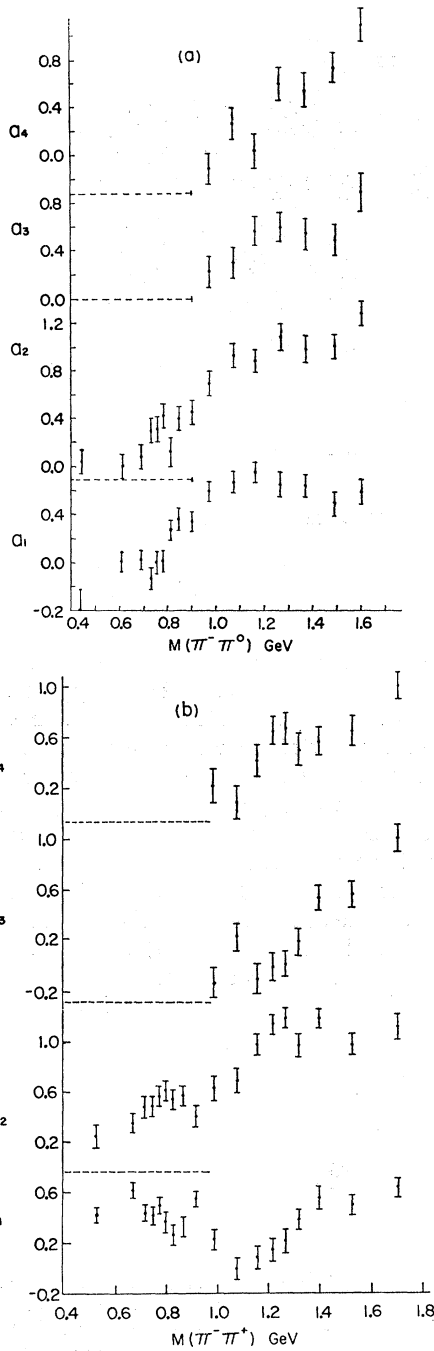(a) $\pi^-\pi^0 p$, (b) $\pi^-\pi^+ n$.

FIG. 12. The coefficients a_i for the best fit to the decay angular distribution $W(\theta) = \frac{1}{2} + \sum_{i=1}^{n} a_i p_i$ for $\Delta^2 \leq 30\mu^2$, where p_i are Legendre polynomials: (a) $\pi^-\pi^0 p$, (b) $\pi^-\pi^+ n$.

TABLE III. Resonance-production cross sections for the states $\pi^-p\pi^0$ and $\pi^-\pi^+n$.

Final state	Resonance	Fraction	Cross section[a] (μb)
$\pi^-p\pi^0$	ρ^-	31.0±1.7	585±32
	$\Delta^+(1236)$	9.0±0.7	169±13
	$N^{*+}(1400)$	4.4±0.7	83±12
	$N^{*+}(1670)$	2.5±0.7	46±13
	$N^{*0}(1670)$	3.3±0.7	62±13
$\pi^-\pi^+n$	ρ^0	40.4±1.7	1152±47
	f^0	18.6±2.0	531±56
	$\Delta^+(1236)$	1.6±0.7	46±20
	$N^{*+}(1400)$	3.6±0.6	103±18
	$N^{*+}(1670)$	2.5±0.5	71±15

[a] The cross sections correspond only to the observed decay modes.

energy-independent Breit-Wigner shapes, with nominal[24] widths and peak positions, for the nucleon isobars, corresponding to obvious bumps in the plots. The fraction of each isobar was obtained. The best fits are shown in the form of smooth curves in Figs. 8 and 9. Table III gives the fraction and the corresponding cross section for each of the observed resonances. The cross sections correspond only to the decay modes observed in the experiment. The contribution denoted by $N^*(1670)$ may be a result of more than one isobar present in that region.[24]
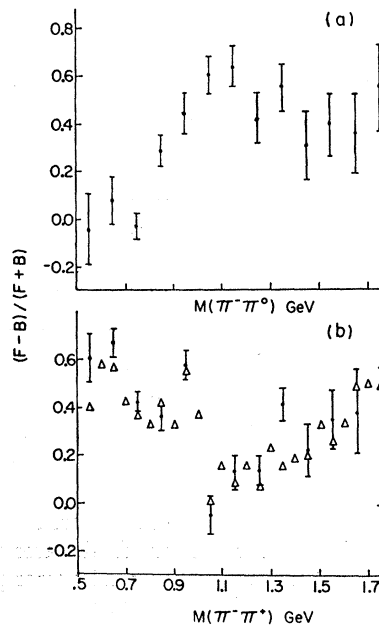

FIG. 13. Forward-backward decay asymmetry as a function of $\pi\pi$ invariant mass for $\Delta^2 \leq 15\mu^2$: (a) $\pi^-\pi^0 p$, (b) $\pi^-\pi^+ n$. In (b) open triangles represent the results of a compilation (see text).

were used to modify the corresponding πN phase spaces. For example, the "modified phase space" for $\pi^+ n$ or $\pi^- n$ in the $\pi^-\pi^+ n$ final state consists of 40.4% ρ^0 reflection, 18.6% f^0 reflection, and 41.0% pure phase space.

Each πN mass spectrum (Figs. 8 and 9) was then fitted to the corresponding "modified phase space" plus

[24] A. H. Rosenfeld, A. Barbaro-Galtieri, W. J. Podolsky, L. R. Price, P. Soding, C. G. Wohl, M. Roos, and W. J. Willis, Rev. Mod. Phys. 39, 1 (1967).
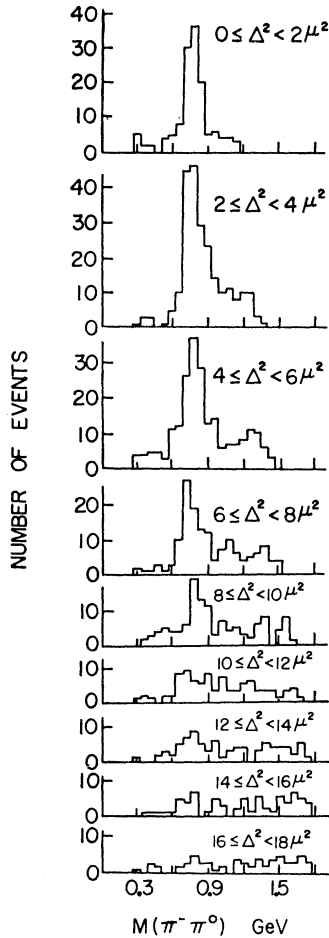
FIG. 14. $\pi\pi$ invariant mass for the state $\pi^-\pi^0 p$ for various intervals of Δ^2.

FIG. 15. Dalitz plot for the state $\pi^-\pi^0 p$ for events with $\Delta^2 < 10\mu^2$.

with the normalization condition

$$\int_0^\pi W(\theta) \sin\theta d\theta = 1.$$

Because of the orthogonality of the Legendre polynomials the coefficients do not change appreciably when the order of the expansion is increased from n to $n+1$. This makes it possible to determine the order of the fit.

Events from the final states $\pi^-p\pi^0$ and $\pi^-\pi^+n$ with $\Delta^2 < 30\mu^2$ were divided, respectively, into groups of 100 and 150 each in ascending order of the $\pi\pi$ mass. The angular distribution in each band was fitted to Eq. (9). Figure 12 shows the results of the maximum-likelihood estimates of the a_i as a function of dipion mass. The χ^2 probabilities of the fits to Eq. (9) are typically 40%.

Up to 1 GeV, $n=2$ is sufficient to describe the data for both the states. The following features are note-
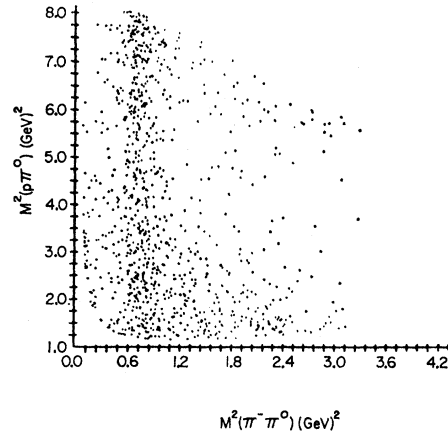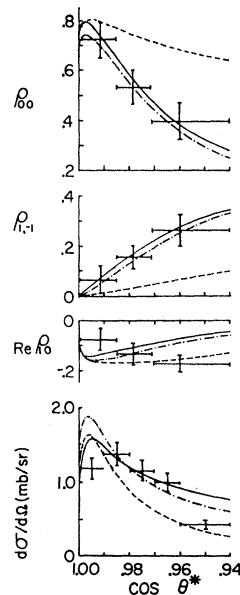
B. Angular Correlations

The importance of decay angular distributions is well known for revealing the nature of the production mechanism. They are studied most conveniently in the t channel with the coordinate system defined below.[23] In the rest frame of the final-state pions, the direction of the incident pion is taken as the z axis, the normal to the production plane $(\hat{n} = \hat{N}_{out} \times \hat{\pi}_{in})$ as the y axis, and $(\hat{y} \times \hat{z})$ as the x axis. In this coordinate system θ is the polar angle of the final-state π^- and φ is the corresponding azimuthal angle.

The scatter plots of $\cos\theta$ and φ versus $M(\pi\pi)$ for events with $\Delta^2 < 20\mu^2$ for both the final states are shown in Figs. 10 and 11. Figure 10(b) exhibits strong forward-backward asymmetry of the ρ^0 decay.

To obtain a more quantitative picture, the dipion decay angular distribution was fitted to an expansion of Legendre polynomials,

$$W(\theta) = \tfrac{1}{2} + \sum_{i=1}^n a_i p_i, \qquad (9)$$

FIG. 16. Spin-density matrix elements and differential cross section for $\rho^-(0.70 \leq M(\pi^-\pi^0) \leq 0.82$ GeV). The dashed, dash-dotted, and solid curves represent absorption model predictions for $\xi = 0$, $\xi = -0.44$, and $\xi = 0.5$, respectively.
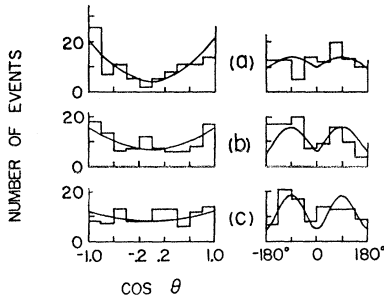
FIG. 17. ρ^- $\cos\theta$ and φ distributions as a function of $\cos\theta^*$: (a) $1.0 \geq \cos\theta^* > 0.985$, (b) $0.985 \geq \cos\theta^* > 0.97$, (c) $0.97 \geq \cos\theta^* > 0.94$. The smooth curves represent the predictions of the absorption model for $\xi = 0.5$.

worthy in the ρ region: (a) The coefficient a_2 exhibits the expected resonancelike behavior; (b) the coefficient a_1, which is a measure of the forward-backward asymmetry, is about zero for $\pi^-\pi^0$ and ~ 0.4 for $\pi^-\pi^+$.

Above 1 GeV, order 4 is sufficient for either state except for the last data point. In Fig. 12(b) the coefficient a_4 shows a peak around 1.25 GeV, as expected from the presence of the spin-2 f^0 meson.

More commonly, the forward-backward asymmetry is defined as $(F-B)/(F+B)$, where F is the number of events with $\cos\theta > 0$ and B is the number with $\cos\theta < 0$. The variation of this asymmetry, for events with $\Delta^2 < 15\mu^2$, as a function of $\pi\pi$ mass is shown in Fig. 13. A compilation[25] of $(F-B)/(F+B)$ ratio for the state $\pi^-\pi^+$, for events with $\Delta^2 < 15\mu^2$, is shown in the form of
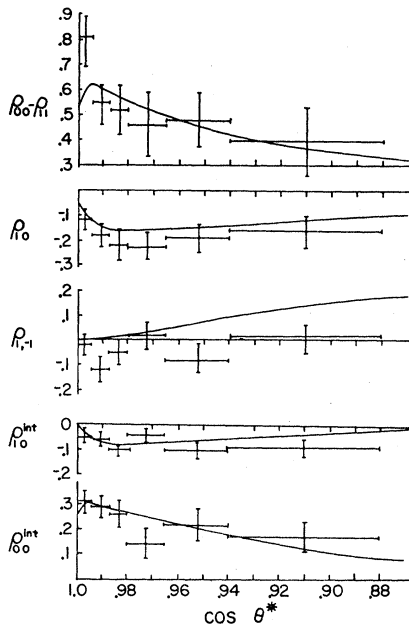

FIG. 18. Spin-density matrix elements for ρ^0 $[0.70 \leq M(\pi^-\pi^+) \leq 0.84$ GeV$]$. The smooth curves represent the predictions of OPEA for $\eta = 0.33$.

[25] J. Veillet, Ecole Polytechnique, Paris (unpublished); see Fig. 7-60 of Ref. 9.

open triangles in Fig. 13(b). The agreement with our data is remarkably good. The asymmetry, which has an average value of about 0.35 in the ρ^0 region, reduces to about 0.15 as the f^0 region is approached.

C. ϱ^- Meson

The one-pion-exchange (OPE) model modified to include absorption[12-15] (OPEA) has been quite successful in predicting the production and decay angular distributions of the $\rho^\pm$ from the reaction $\pi^\pm + p \rightarrow \rho^\pm + p$ at a number of incident beam momenta.

In order to test the validity of OPEA, one needs a "clean" sample of ρ^-. This can be achieved by restricting to small values of Δ^2, as is obvious from Fig. 14, which depicts the variation of the $\pi^-\pi^0$ mass spectrum with Δ^2. From the figure we see that the background under the ρ peak starts increasing for $\Delta^2 > 10\mu^2$. Therefore, for the purpose of analysis we restrict ourselves to events with $\Delta^2 < 10\mu^2$ and $M(\pi^-\pi^0)$ between 0.70 and 0.82 GeV. There are 304 events which meet these criteria.[26]

However, these events may still have some contamination from $\Delta^+(1236)$. One can obtain an estimate of this contamination from the Dalitz plot for $\Delta^2 < 10\mu^2$ (Fig. 15). There are 27 events in the overlap region of
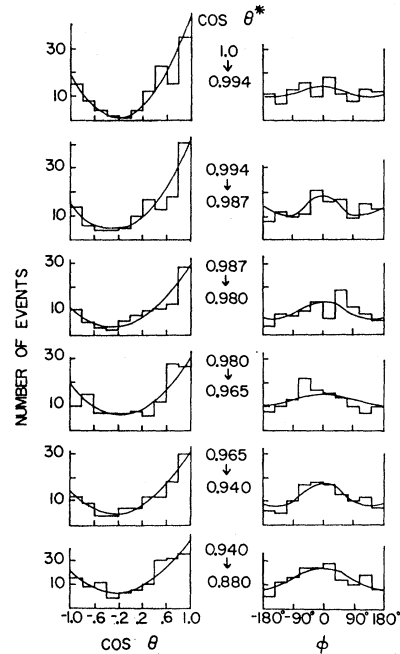

FIG. 19. ρ^0 $\cos\theta$ and φ distributions as a function of $\cos\theta^*$. The smooth curves represent the predictions of OPEA for $\eta = 0.33$.

[26] Note that $\Delta^2 < 10\mu^2$ corresponds to $p_+ < 455$ MeV/c, which is well within the limit (1300 MeV/c) for visible ionization identification. Therefore, this sample has no contamination from hypothesis (2). Fitting the $\pi^-\pi^0$ mass spectrum for $\Delta^2 < 10\mu^2$ to a combination of phase space and a Breit-Wigner shape for ρ^-, we find that the background in these 304 events is no more than 8%.

the ρ^- and the Δ^+ bands. Following the suggestion of Eberhard and Pripstein[27] the overlap region was repopulated with corresponding "conjugate events." It was found, however, that the analysis presented below gives the same results with or without the repopulation of the overlap region.

These events were divided into three groups of about 100 each in descending order of $\cos\theta^*$. For each group the best fit to

$$W(\theta,\varphi) = \frac{3}{4\pi} [\rho_{00} \cos^2\theta + \tfrac{1}{2}(1-\rho_{00}) \sin^2\theta$$

$$-\rho_{1,-1} \sin^2\theta \cos 2\varphi - \sqrt{2} \operatorname{Re}\rho_{10} \sin 2\theta \cos\varphi] \quad (10)$$

was determined using the program MINFUN and the unknown parameters $\rho_{00}, \rho_{1,-1}$, and $\operatorname{Re}\rho_{10}$ were obtained (Fig. 16).

Many authors[12-15] have calculated the values of the density matrix elements[28] for $\rho^\pm$ decay assuming OPEA. The predictions[29] of OPEA for this energy are shown by dashed curves in Fig. 16. The discrepancy[30] between our results and OPEA is quite apparent. This discrepancy leads us to include some contribution from vector meson exchange. The analysis with more details has been reported earlier.[17] It was found that the best fit to these data is obtained when $|\xi| \simeq 0.5$, where

$$\xi = \frac{g_{\pi\rho\omega}(G_{\omega\bar{p}p}^V + G_{\omega\bar{p}p}^T)}{2g_{\pi\pi\rho}G_{\pi\bar{p}p}} \quad (11)$$

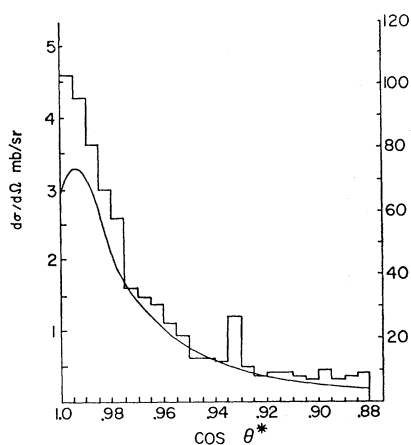measures the relative strength of ω to π exchange[12] (superscripts V and T stand for vector and tensor

FIG. 20. Differential cross section for ρ^0 production. The smooth curve represents the predictions of OPEA for $\eta=0.33$.

FIG. 21. Cross section for the reaction $\pi^-p \to n f^0 (f^0 \to \pi^-\pi^+)$ as a function of π^- beam momentum. ●—Ref. 1; ○—Ref. 37; ▲—This experiment; △—Our estimates for Ref. 38; ■—Ref. 39.

coupling). In Fig. 16, dashed, dash-dotted, and solid curves represent calculated values[29] for $\xi=0$, $\xi=-0.44$, and $\xi=0.5$, respectively. The production angular distribution for ρ^- is also shown in Fig. 16.

Integrating expression (10), one gets

$$W(\varphi) = (1/2\pi)[(1+2\rho_{1,-1}) - 4\rho_{1,-1} \cos^2\varphi], \quad (12)$$

$$W(\cos\theta) = \tfrac{3}{4}[(1-\rho_{00}) + (3\rho_{00}-1) \cos^2\theta]. \quad (13)$$

Figure 17 shows the $\cos\theta$ and φ distributions for the 304 events divided into three groups on the basis of $\cos\theta^*$. The predictions of the absorption model for $|\xi|=0.5$ are shown by smooth curves.

D. ϱ^0 Meson

It is well known that the ρ^0 decays asymmetrically. To explain this Durand and Chiu[31] proposed the existence of a $T=0$, S-wave resonance (ϵ^0) near the ρ mass and interpreted the observed asymmetry as an interference between the two resonances. There is more evidence against [32,1] than for[33] the existence of such a resonance. Furthermore, an interference with a non-resonant S wave can also account for the asymmetry.[34] This interpretation has been considered in previous investigations.[7,35,36]

The latter possibility is assumed here. With the inclusion of a $T=0$, $J=0$ amplitude, the "ρ" decay

[27] P. Eberhard and M. Pripstein, Phys. Rev. Letters 10, 351 (1963).

[28] K. Gottfried and J. D. Jackson, Nuovo Cimento 33, 309 (1964).

[29] The predictions were computed by using a program by R. Keyser, CERN Report No. DD/CO/66/3 (unpublished).

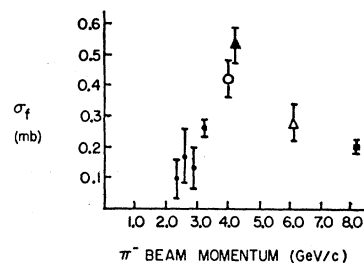[30] A similar discrepancy was observed at 8 GeV/c by I. Derado et al. (Ref. 11).

[31] L. Durand, III and Y. T. Chiu, Phys. Rev. Letters 14, 329 (1965).

[32] H. O. Cohn, W. M. Bugg, G. T. Condo, R. D. McCulloch, G. Lutjens, and N. Gelfand, Phys. Rev. Letters 15, 906 (1965); R. J. Miller, S. Lichtman, F. J. Loeffler, and R. B. Willmann, Bull. Am. Phys. Soc. 12, 10 (1967); M. A. Jabiol, F. E. James, and N. H. Khanh, Phys. Rev. Letters 17, 1065 (1966); I. F. Corbett, C. J. S. Damerell, N. Middlemas, D. Newton, A. B. Clegg, W. S. C. Williams, and A. S. Carroll, Phys. Rev. 156, 1451 (1967).

[33] M. Feldman, W. Frati, J. Halpern, A. Kanofsky, M. Nussbaum, S. Richert, P. Yamin, S. Choudry, S. Devons, and J. Grunhaus, Phys. Rev. Letters 14, 869 (1965); V. Hagopian, W. Selove, J. Alitti, J. P. Baton, and M. Neveu-René, ibid. 14, 1077 (1965).

[34] M. M. Islam and R. Pinon, Phys. Rev. Letters 12, 310 (1964); S. H. Patil, Phys. Rev. Letters 13, 261 (1964); P. G. Turnauer, ibid. 14, 985 (1965).

[35] W. D. Walker, J. Carroll, A. Garfinkel, and B. Y. Oh, Phys. Rev. Letters 18, 630 (1967).

[36] M. Bander and G. L. Shaw, Phys. Rev. 155, 1675 (1967); D. Griffiths and R. J. Jabbur, Phys. Rev. 157, 1371 (1967).

angular distribution may be written as

$$W(\theta,\varphi) = \tfrac{1}{4}\pi + \tfrac{3}{4}\pi\{ (\rho_{00}-\rho_{11})(\cos^2\theta - \tfrac{1}{3})$$
$$-\sqrt{2}\ \mathrm{Re}\rho_{10}\ \sin 2\theta\ \cos\varphi - \rho_{1,-1}\sin^2\theta\ \cos 2\varphi\}$$
$$+ (\sqrt{3}/4\pi)\{ -2\sqrt{2}\ \mathrm{Re}\rho_{10}{}^{\mathrm{int}}\ \sin\theta$$
$$\times\cos\varphi + 2\ \mathrm{Re}\rho_{00}{}^{\mathrm{int}}\ \cos\theta\}, \quad (14)$$

where ρ^{int} denote the density matrix elements for S-P interference.

For the determination of the density matrix elements we limit the analysis to 717 events with $\pi^-\pi^+$ mass between 0.70 and 0.84 GeV and $\Delta^2 < 20\mu^2$. These events were divided into six nearly equal groups in descending order of $\cos\theta^*$. Using a maximum-likelihood method, the experimental decay angular distribution was fitted to expression (14). The results are shown in Fig. 18.

To obtain the theoretical predictions of OPEA for a mixture of P- and S-wave production, one requires the knowledge of the strength of the $\pi\pi$ S-wave interaction relative to the $\pi\pi$ P-wave interaction: $\eta = f_{\pi\pi S}/g_{\pi\pi P}$ (where $f_{\pi\pi S}$ is related to the average value of the S-wave amplitude in the ρ region). The predictions of OPEA were calculated[29] for various values of η. The best agreement with the data was obtained for $\eta \approx 0.33$ (solid curves in Fig. 18).

Integrating equation (14), one obtains the polar and azimuthal decay angular distributions:

$$W(\cos\theta) = \tfrac{1}{2}\{1 + (\rho_{00}-\rho_{11})(3\cos^2\theta - 1)$$
$$+ 2\sqrt{3}\ \mathrm{Re}\rho_{00}{}^{\mathrm{int}}\ \cos\theta\}, \quad (15)$$

$$W(\varphi) = 1/2\pi\{1 + \rho_{1,-1}(1 - 2\cos^2\varphi)$$
$$- (\tfrac{1}{2}\pi\sqrt{6})\ \mathrm{Re}\rho_{10}{}^{\mathrm{int}}\ \cos\varphi\}. \quad (16)$$

The corresponding experimental distributions for each of the six groups of events are displayed in Fig. 19. Figure 20 shows the production angular distribution. The theoretical predictions with the inclusion of a non-resonant interfering S-wave for $\eta = 0.33$ are shown by smooth curves in both the figures.

E. f^0 Meson

This experiment is particularly well suited for an analysis of the f^0 meson. Figure 21 depicts the behavior
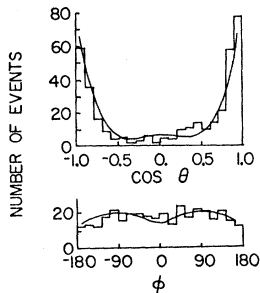

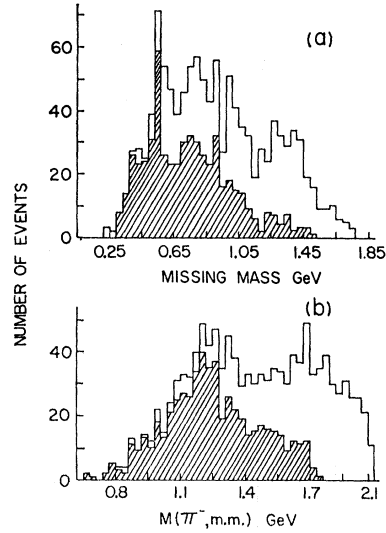FIG. 22. $\cos\theta$ and φ distributions of f^0 for events with $\Delta^2 \le 20\mu^2$.

FIG. 23. Invariant-mass plots for the reaction $\pi^- p \to \pi^- p$ +m.m. (a) Missing mass; (b) $M(\pi^-,\mathrm{m.m.})$. The shaded area represents events with $\Delta^2(p \to p) < 15\mu^2$.

of the f^0 production cross section from reaction (2) as a function of π^- beam momentum.[37-39] The present experiment appears to be situated near the peak in Fig. 21. It was hoped that the large cross section and the improved statistics of this work would allow a thorough analysis of this resonance.

The f^0 decay angular distribution is expressed in terms of its density matrix elements as

$$W(\theta,\varphi) = (15/16\pi)\{3\rho_{00}(\cos^2\theta - \tfrac{1}{3})^2$$
$$+ 4\rho_{11}\sin^2\theta\ \cos^2\theta + \rho_{22}\sin^4\theta - 2\cos\varphi$$
$$\times\sin 2\theta\ [\mathrm{Re}\rho_{21}\sin^2\theta + (\sqrt{6})\ \mathrm{Re}\rho_{10}(\cos^2\theta - \tfrac{1}{3})]$$
$$- 2\cos 2\varphi\ \sin^2\theta[2\rho_{1,-1}\cos^2\theta - (\sqrt{6})\ \mathrm{Re}\rho_{20}$$
$$\times (\cos^2\theta - \tfrac{1}{3})] + 2\ \mathrm{Re}\rho_{2,-1}\cos 3\varphi\ \sin^2\theta\ \sin 2\theta$$
$$+ \rho_{2,-2}\cos 4\varphi\ \sin^4\theta\}, \quad (17)$$

with the trace condition

$$\mathrm{Tr}(\rho) = \rho_{00} + 2\rho_{11} + 2\rho_{22} = 1. \quad (18)$$

To determine the f^0 density matrix elements, events with $1.18 \le M(\pi^-\pi^+) \le 1.32$ GeV and $\Delta^2 \le 20\mu^2$ were used. The experimental decay angular distribution was fitted to Eq. (17) by a maximum-likelihood technique.

[37] L. Bondar, K. Bongartz, M. Deutschmann, H. Weber, D. C. Colley, W. P. Dodd, J. Simmons, B. Tallini, J. Moebes, B. Nellen, G. Winter, E. Lohrmann, E. Raubold, G. Wolf, J. M. Brownlee, I. Butterworth, F. I. Campayne, M. Ibbotson, Y. S. Liu, N. N. Biswas, I. Derado, D. Luers, G. Lutzens, and M. Schmitz, Phys. Letters 5, 153 (1963).

[38] J. J. Veillet, J. Hennessy, H. Bingham, M. Bloch, D. Drijard, A. Lagarrique, P. Mittner, A. Rousset, G. Bellini, M. de Corato, E. Fiorini, and P. Negri, Phys. Rev. Letters 10, 29 (1963).

[39] N. N. Biswas, N. M. Cason, I. Derado, V. P. Kenney, J. A. Poirier, W. D. Shephard, and E. H. Synn, University of Notre Dame report, 1966 (unpublished).
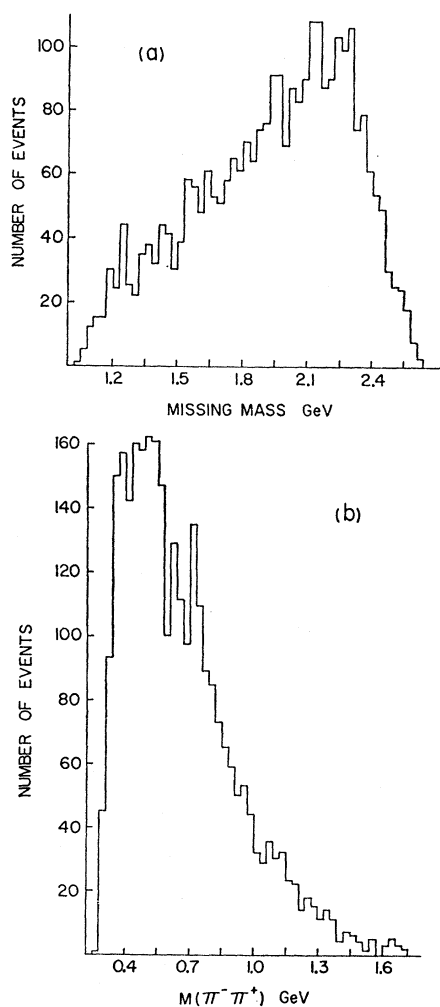
FIG. 24. Invariant-mass plots for the reaction $\pi^-p \to \pi^-\pi^+ + $m.m.
(a) Missing mass; (b) $M(\pi^-\pi^+)$.

The results obtained are as follows:

$$\rho_{22} = -0.21 \pm 0.02, \quad \rho_{2,-1} = 0.01 \pm 0.01,$$

$$\rho_{11} = 0.26 \pm 0.02, \quad \rho_{2,-2} = -0.01 \pm 0.02,$$

$$\rho_{21} = -0.06 \pm 0.01, \quad \rho_{10} = -0.10 \pm 0.02,$$

$$\rho_{20} = 0.01 \pm 0.01, \quad \rho_{1,-1} = 0.09 \pm 0.02,$$

Figure 22 shows the experimental $\cos\theta$ and φ distributions for the same sample of events. The smooth curves are obtained by substituting the values of the density matrix elements into θ and φ projections of Eq. (17).

The depopulation of events near $\cos\theta = 0$ leads to the negative value of ρ_{22}, a result which has been observed in previous investigations.[40,41]

It is impossible for any diagonal element of the f^0 density matrix to be negative. Consequently, background under the f^0 must significantly affect the values of the density matrix elements. An analysis of possible background contribution is now underway.

V. FINAL STATES $\pi^-p \to \pi^-p + $NEUTRALS AND $\pi^-p \to \pi^-\pi^+ + $NEUTRALS

A total of 15 538 events were assigned to these final states. From a subsample of 5496 events, 4185 with $p_+ < 1300$ MeV/c were examined for ionization identification. 1246 events were consistent with hypothesis (4) and 2939 with hypothesis (5).

In this section we present the results of the study of $\pi^-p \to \pi^-p + $missing mass (m.m.) [reaction (4)] and $\pi^-p \to \pi^-\pi^+ + $m.m. [reaction (5)] based on 1246 and 2939 events, respectively. These numbers do not include contributions from 1311 events with $p_+ > 1300$ MeV/c and therefore form biased samples.

Figure 23 shows missing mass and $M(\pi^-,$m.m.$)$ plots for reaction (4). The shaded area represents events with $\Delta^2 \leq 15\mu^2$. The presence of a narrow η peak is quite striking. One also observes an excess of events in the ω region. In Fig. 23(b) the enhancement near 1.2 GeV may be due to the B meson.

Missing mass and $M(\pi^-\pi^+)$ plots for reaction (5) are shown in Fig. 24. There is some evidence for ρ^0 production [Fig. 24(b)].

ACKNOWLEDGMENTS

The authors would like to express their gratitude to the Lawrence Radiation Laboratory for providing the film. We want to thank the scanning and measuring crew under the supervision of Mrs. B. Clark for their cooperation and care in the film analysis. We also thank Professor C. H. Chan, Professor L. J. Gutay, and Professor T. R. Palfrey, Jr., for various discussions and valuable criticism and Professor T. H. Groves for participation in the early stages of the experiment.

[40] Aachen-Berlin-CERN Collaboration, Phys. Letters **22**, 533 (1966).
[41] H. Cohn, R. D. McCulloch, W. M. Bugg, and G. T. Condo, Nucl. Phys. **82**, 690 (1966).